Proceedings of the
Annual Stability Conference
Structural Stability Research Council
Atlanta, Georgia, April 21-24, 2020

Investigation on the stability behavior of cold-formed steel beam-column members under bi-axial bending

Sevugan Rajkannu J[1], Arul Jayachandran S.[2]

Abstract

This paper presents the experimental and numerical investigations on the cold-formed steel beam-column members under bi-axial loading. In this study, the lipped channel cross-section of members are considered for the investigation on the cross-sectional and global buckling effects on the strength of the member. Experiments are conducted by applying an eccentric compression to create axial load and a moment gradient. Carefully designed experiments are carried out so that the member will be subjected to uniform and non-uniform moments throughout the member. The influence of varying moment on the various buckling behavior is examined. The use of moment correction factor (C_b) in the case of FTB and distortional buckling is discussed. The study presents the influence of moment amplification factor (C_m) on the strength prediction. A study is also carried out using ABAQUS, which is then validated with the experimental results. The numerical model is extended to study the behavior of a spectrum of axial and bending combinations. The results from the experiment and numerical model are compared with the code specification AISI S100-16 for DSM design both for the linear interaction (LI) framework and the non-linear interaction (NLI) framework. The results show that the LI framework predicts strength conservatively by 30 to 90% for biaxial bending. The details of the study is presented in this paper.

1. Introduction

The behavior of open section members under combined axial loading and bending moments is complicated because it involves rotation due to bending and deformation due to axial load and also twisting of the member due to loading and symmetry of the cross-section (Chen and Atsuta 1976). Based on the slenderness ratio and type of failure, the ultimate strength of beam-column members is calculated using different linear interaction equation (i) strength equation, and (ii) stability equation. The Study of (Sohal et.al.1989) Shows the weakness of using the two interaction equation for finding the strength of the member and proposed the need for a single equation.

[1] Research Scholar, Indian Institute of Technology Madras, India, <sevuganrajkannu@gmail.com>
[2] Professor, Indian Institute of Technology Madras, India, aruls@iitm.ac.in

To understand the behavior of beam-column under combined bending and compression (Galambos, 1960) conducted a series of experiments on I-sections under biaxial loading. For members with thin-walled sections, the behaviour is still more complicated because thin-walled cold-formed steel (CFS) structural members are often sensitive to instabilities at the element level (local buckling), the cross-section level (distortional buckling), and the member level (global buckling).

Design of CFS members using current design specifications such as AISI S100 or AS/NZS 4600 formally provide the traditional effective width method (EWM) and the direct strength method (DSM) to determine the member axial load and bending moment capacities (AISI 2016; Standards Australia 2005). Combined actions on a member are taken into account through a simple linear interaction of pure axial or flexural strength, as shown in Eq.(1). The axial strength (P_n), flexural strength (M_{nx}, M_{ny}) of the member calculated separately using EWM or DSM are applied in the linear interaction shown in Eq. (1).

$$\frac{P}{P_n}+\frac{C_{mx}M_x}{\alpha_x M_{nx}}+\frac{C_{my}M_y}{\alpha_y M_{ny}}\leq 1 \tag{1}$$

Where C_{mx}, C_{my} is the moment gradient factor. α_x, α_y is the moment amplification factor to account for second-order effects.

$$C_{mx}=0.6-0.4\frac{M_1}{M_2} \tag{2}$$

$$\alpha_x=\left(1-P\big/P_{ex}\right) \tag{3}$$

where M_1, M_2 are the end moments and P_{ex}, P_{ey} are the Euler buckling loads about the major and minor axes. However, the original representative interaction equation is not linear (Schafer 2006). To produce safe and economical design guidelines, the actual relationship for combined bending and compression about their two principal cross-sectional axes requires further investigation.

The capacity of cold-formed steel beam-column bending about one of their principal axis has been widely studied by (Pekoz and Winter 1969), (Miller and Pekoz 1994), (Rasmussen, 2006). The study on in-plane buckling behaviour of the lipped channel section under beam-column action (Li et.al., 2016) shows that there is a need for modification on the implementation of the second-order effects. Test results of (Kalyanaraman and Rao 1998) on beam-column show the influence of combined stress action in CFS beam-column prediction. However, a fewer studies have investigated the members under biaxial bending behaviour of the CFS section. (Shanmugam et.al.,1989) conducted an experimental study on the box section under combined axial and biaxial bending. The behavior of CFS member under pure biaxial bending was studied experimentally in (Put et.al., 1999; Talebian et.al., 2018).

A nonlinear interaction framework (NLI), in terms of β, θ_{mm}, and ϕ_{pm} is proposed by (Schafer, 2012). To validate the DSM formulation of nonlinear interaction, 54 experiments (Torabian et.al., 2014) were conducted on the lipped channel section of 600S137-54 with uniform moment throughout the member. Application of nonlinear interaction to Z –section beam-column is reported in (Torabian et.al, 2015). The series of beam-column experiments on rack section

(Vijayavengadesh Kumar and Arul Jayachandran 2016) shows the NLI is unconservative for a linearly varying moment, and also pointed out that the proper usage of θ_{MM} and ϕ_{PM} corresponding to $M_{2y,min,}$ and $M_{2y,max}$ values to be used in the nonlinear interaction format.

The beam-column capacities under moment gradient were studied in (Chen and Atusta 1975) Experiments by (Galambos 1960) are some of the few experimental validations for the varying moment factors. (Pillai, 1981) shows that the extension of linear interpolation of two uniaxial bending cases for biaxial bending is a conservative simplification. It is added that the equivalent moment factor C_m originally developed for uniaxial bending is extended to biaxial bending also. The study of (Chen and Zhou, 1988) shows that equivalent moment factor (C_m) on the beam-column design developed based on the elastic analysis from hot rolled I-section and box section, which provides a close approximation for inelastic range also. The study of (Sevugan Rajkannu and Arul Jayachandran, 2018) on the effect of moment gradient on major axis bending showed the effect of the implementation of varying moment factor on the new Non-linear interaction framework.

From the literature, it is clear that the test results on beam-column members with biaxial bending is very less. The studies on the effect of moment gradient on the biaxial-bending member is still scarce. This paper presents the experimental results on the lipped channel member under biaxial bending with uniform and varying moments. Two different lengths of the member were selected for the study. With the limited experimental results, the study is extended to the numerical study validated with the experimental results. Extensive numerical study on two different lengths of member are conducted, to study the influence of varying moment on global and distortional buckling strength under beam-column action. The results from the experiment and numerical studies are compared with the linear interaction equation currently considered in AISI S100-2016 and newly developed non-linear interaction equation framework.

2. Experimental study

2.1 Tested specimen

The specimen tested is a lipped channel cross-section of dimension given in Fig (1b). Two lengths of the member are selected for the study (1600 mm and 750 mm length). Fig. 1a) shows the signature curve for the selected lipped channel cross-section under axial compression. A member length of 1600 mm is expected to buckle in flexural torsional buckling (FTB), and a 750 mm length member may undergo distortional buckling under axial compression.

The member under compression and biaxial bending only are explained in this study. Based on the loading, specimens are classified into two series. (i) bi-axial compression with the uniform moment, as shown in Fig (2 a) (ii) bi-axial compression with varying moment as shown in Fig (2b). The tested specimen is represented based on the length and loading type, which is represented as 750 or 1600 (length of a member), B represents the biaxial loading and (U or V) for uniform and varying moment respectively.

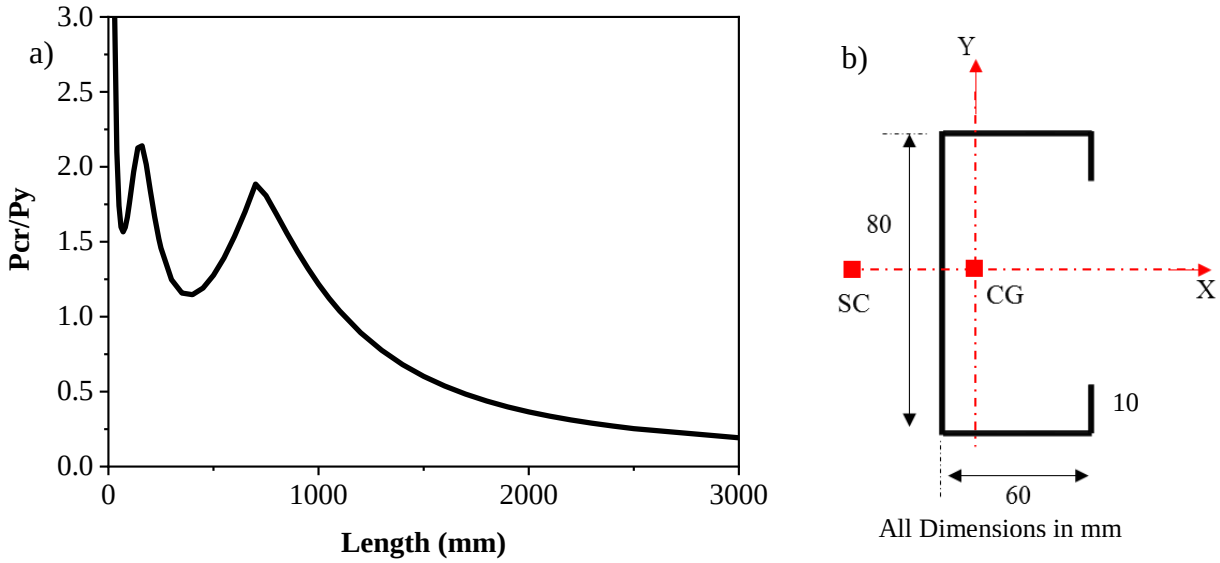

Figure 1: a) Signature curve of the selected specimen b) Dimensions of the selected lipped channel section

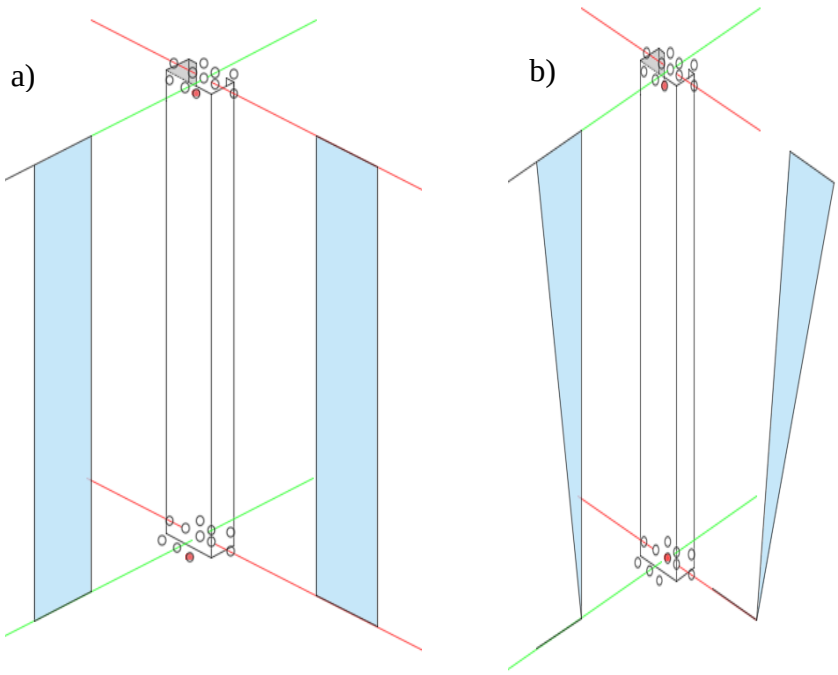

Figure 2: a) Uniform Moment b)Varying moment

2.2 Material property

The tension coupons are prepared based on the recommendation of ASTM A-370 and (Huang and Young, 2014). The coupon tests are carried in a displacement controlled universal testing machine. The loading rate adopted for testing is 0.05 mm/minute up to yielding, and 0.8 mm/minute after yielding. The specimen is kept for relaxation for 5 minutes after yielding. Strain gauges are placed on both the sides of the coupon. The average strain from the strain gauge is used for the calculation of Young's modulus. The material properties such as yield stress, ultimate stress, and Young's modulus are summarized in Table 1. The average yield stress value is 238 MPa. Fig. 3 shows the plot of stress vs. strain for the coupons.

Table 1: Tension Coupon test results

Test	Yield Stress (MPa)	Ultimate Stress (MPa)	Young's Modulus (GPa)
1	230	332	191.5
2	236	338	199.3
3	237	339	209.9
4	250	353	205.5
Mean	238.2	340.5	201.5

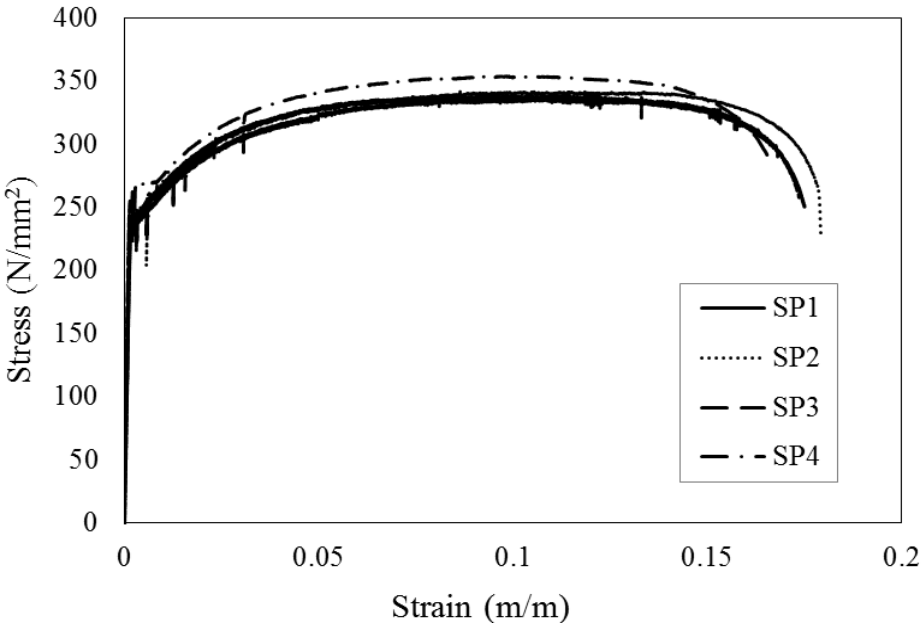

Figure 3: Tensile stress-strain curve of the specimen

2.3 Test setup and procedure

The specimen is welded to an end plate such that centroid of cross-section and centroid of the plate are in the same axis. Thus the endplate won't allow any warping deformation at the ends. A hardened plate is made with an indentation at the center of gravity of plate and at points of desired application of load eccentricity. The advantages of this fixture are that the load can be applied eccentrically to both the axes resulting in the biaxial moment with uniform and moment gradient along the length. To arrest torsional displacements, a small fixture is made such that it allows major axis bending and minor axis rotation while arresting the torsion. The specimen is carefully placed on the test setup on the spherical balls so that the required loading can be applied. The overall test setup and instrumentation adopted is shown in Fig. 4. The specimen is tested using the 500 kN MTS actuator with displacement control to capture the post buckling behaviour of the member. The experiments are conducted at a displacement rate of 0.005 mm/sec.

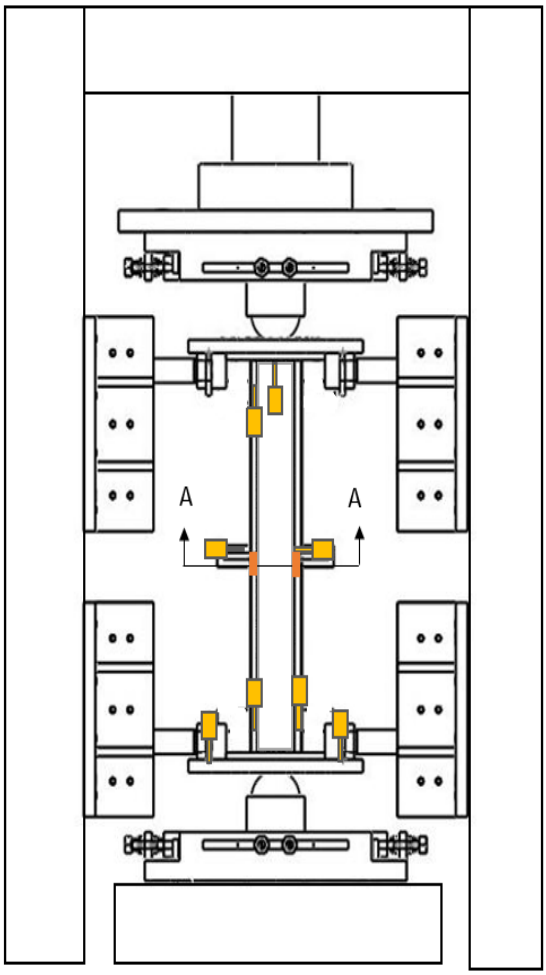

a)

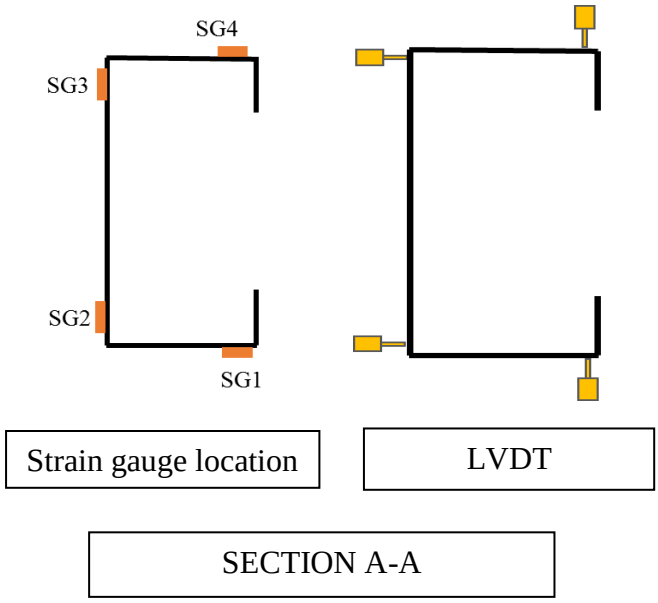

b)

Figure 4: a) Test setup b) Instrumentation scheme (Sevugan Rajkannu and Arul Jayachandran 2019)

Four strain gauges are used to measure the strain at the mid-length of the member. 8 LVDTs are used, of which 4 LVDTs are placed at mid-length to measure the buckling deformation and twist of the cross-section. 2 LVDTs are used at the top and bottom endplates each to measure the rotation.

2.4 Test results

The series of experiments with uniform and moment gradient were performed. In this study, the biaxial loading with 4 tests on the uniform moment. 4 tests on the moment gradient are explained. The test results are compared with the CG loading of the same specimen. The test results from paper (Sevugan Rajkannu and Arul Jayachandran, 2019) is taken for the CG load results of 1600 mm specimen. Each test is repeated twice to check the repeatability of the results.

2.4.1 Bi-axial loading (uniform moment)

The members are subjected to biaxial bending in addition to compression with warping restrained boundary conditions. Because of mono-symmetricity of the cross-section lipped channel section member fails in the combination of the flexural and torsional mode (FTB) under axial compression. Since the member is made of thin sheets of steel, Longer specimen (1600

mm) fails in the interacton of global FTB and distortional buckling under CG loading. The member was subjected to bi-axial eccentricity from the CG axis, as shown in Fig (2a). In the case of longer member (1600 mm), the member started deflecting in both the direction because of the biaxial moment. The eccentricity about the minor axis is positive (away from SC side) and creates compression in the lip of the cross-section. Thus increase in stress in the lip due to compression makes the flange lip to distort. at mid-length of a member. Because of distortion of one lip, and there is a slight twist in the post-peak region finally failed with a combination of global FTB and distortional buckling. Fig. 5 shows the buckling mode for the members under the biaxial-uniform moment along the length. In the case of 750 mm length due to the reduced slenderness ratio, load carrying capacity is increased. In this case also, member deflects about both the axis due to biaxial moment and finally fail due to distortional buckling with outward-outward deformation of the lip, which is clearly shown in Fig (5b). Strain gauge results for the members shown in Fig. 6 indicates that the variation of strain in the elements of cross-section at the mid-length. Fig (6 a) shows the strain reading for 1600 mm length member. Figure depicts that SG2 strain gauge is in tension due to minor axis and major axis bending. SG1 experiences tension due to major axis bending and compression due to minor axis bending and axial compression. SG4 has higher compression compressive strain reaching yield strain due to major axis bending, and axial compression, Whereas other elements are much lesser than yield strain at the same cross-section. Thus the member fails in an elastic region due to high slenderness. However, in the case of a 750 mm length member, the elements of the cross-section are reaching yield strain much before the ultimate load. The cross section is yielded because of lower slenderness ratio and lower yield strength of the material. The failure is mainly due to the combination of yielding and buckling (Inelastic buckling). The ultimate load and failure mode are given in Table 2. From this, it is clear that eccentricity plays an important role in the strength of the member.

Table 2: Test results with failure loads and modes

Specimen name	e_x mm	e_y mm	P_{ult} kN	M_1 kNmm	M_2 KNmm	P/P_y	M_1/M_y	$M2/M_y$	Mode
1600-CG	0	0	53.71	0	0	0.65	0	0	FTB+D
1600-B-U	35	35	13.38	468.47	468.48	0.16	0.19	0.45	D+FTB
750-CG	0	0	64.73	0	0	0.79	0	0	D
750-B-U	35	35	18.45	645.75	645.75	0.22	0.27	0.62	D

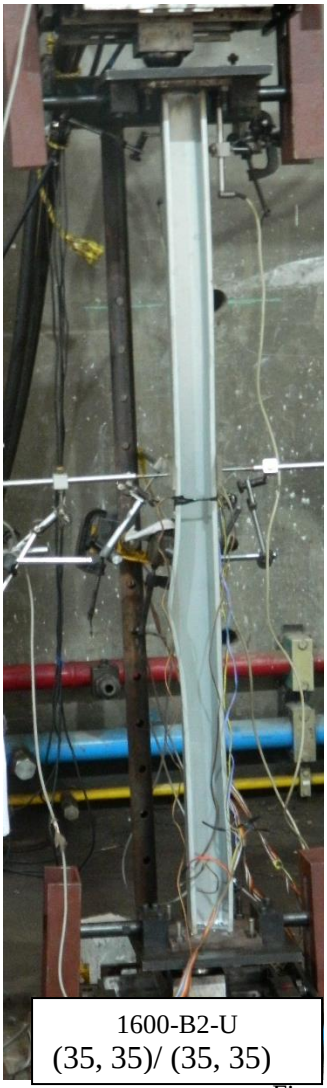

1600-B2-U
(35, 35)/ (35, 35)

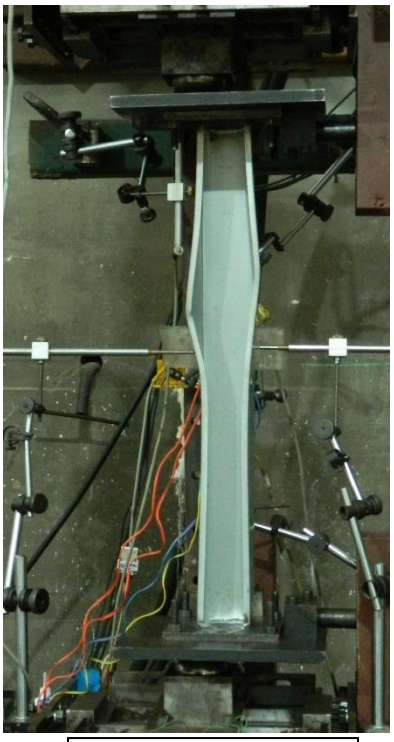

750-B2-U
(35, 35)/ (35, 35)

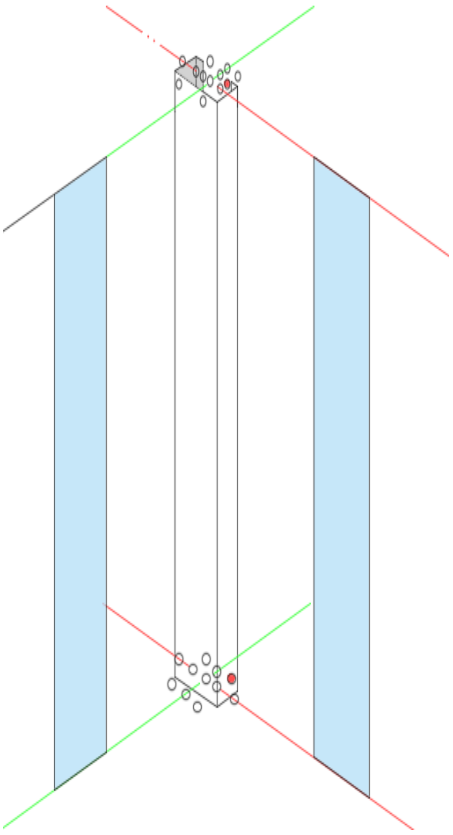

Figure 5: Failure buckling mode shape of under axial compression

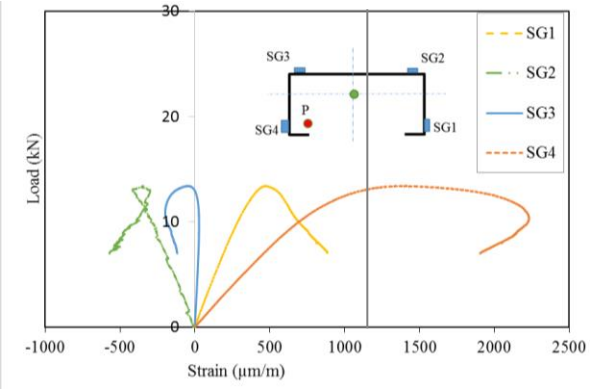

a) 1600-B-U

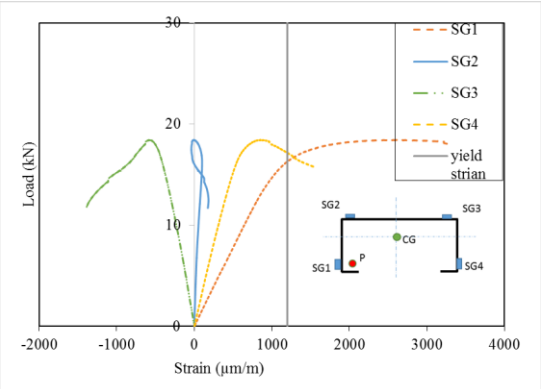

b) 750-B-U

Figure 6: load vs. strain for members under bi-axial loading under the uniform moment

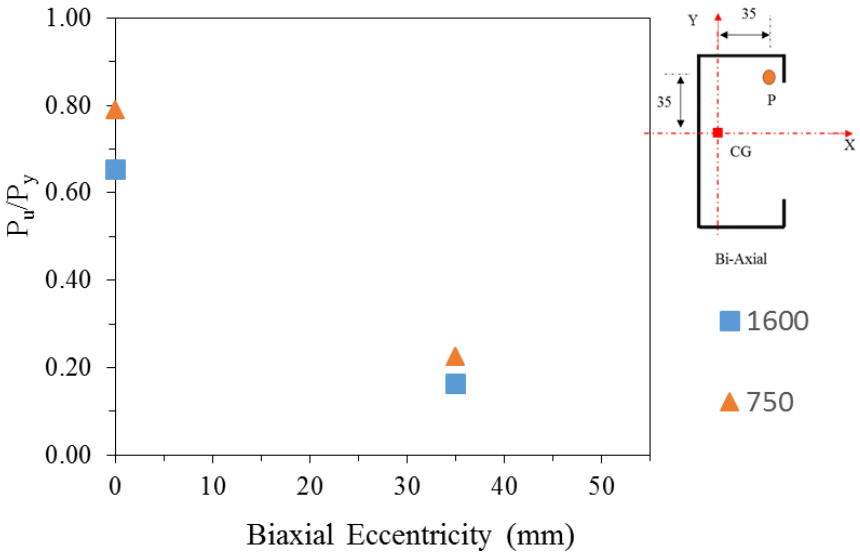

Figure 7: Normalized ultimate load vs Bi-axial eccentricity

2.4.2 Beam-column behavior under moment gradient

The experimental study on the moment gradient in the case of beam-column under biaxial bending is very less in the literature. The varying moment affects the overall capacity and behaviour of the member. Most of the theoretical calculation for buckling equation is derived mainly based on the uniform moment throughout the members. The effect of moment gradient on individual moment capacity for LTB is generally taken care of by the empirical factor, which also determined mostly based on the I section. The moment gradient alters the buckling mode because of the varying stress distribution along the length and cross section.

The behavior of beam-column member mainly depends on the variation of moment and magnitude of moments at the top and bottom of the member. In this study, the moment gradient case shown in Figure (2b) is presented. The one end of the member is loaded at CG, and another end is subjected to biaxial bending. Fig (10) shows the failure modes of the member under a biaxial varying moment. The failure of the member is mainly due to distortional buckling because the positive eccentricity about the minor axis create compression on the lip of the section. The failure is near to the bottom of the member due to moment at the bottom end.. In the case of a 750 mm length member, member failed due to distortional buckling with inward-inward deformation of the flanges. The results of the moment gradient are given in Table (3). There is a marked difference in behavior and ultimate load for the two different lengths of the member. The load carrying capacity due to moment gradient along the member is higher than the uniform moment throughout the length, which clearly shows the effect of the moment gradient.

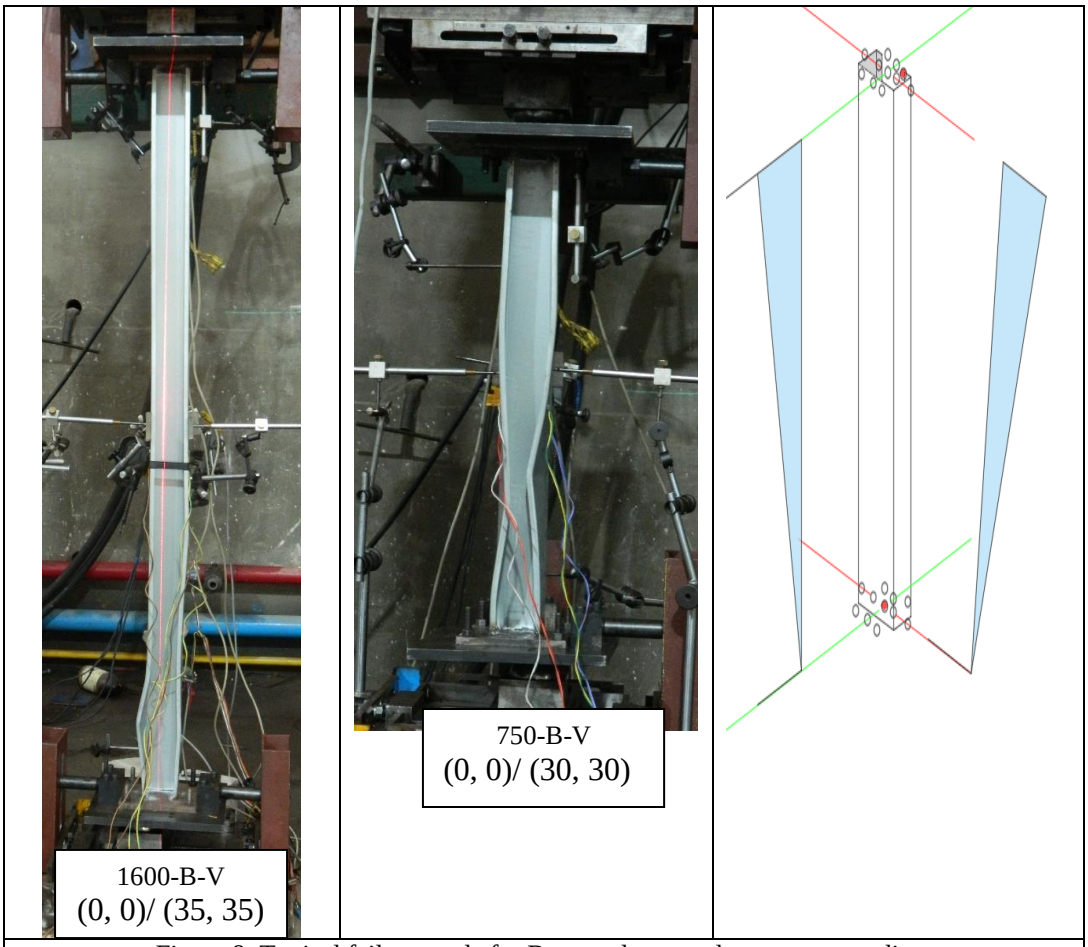

Figure 8: Typical failure mode for Beam column under moment gradient

Table 3: Test results with failure loads and modes

Specimen name	Top e_x mm	Top e_y mm	Bottom e_x mm	Bottom e_y mm	P_{ult} kN	P/P_y	M_{1max}/M_{1y}	M_{2max}/M_{2y}	Mode
1600-B-V	0	0	35	35	18.25	0.22	0.26	0.62	D+FTB
750-B-V	0	0	30	30	29.95	0.36	0.37	0.88	D

3. Numerical study

The numerical modelling is conducted using finite element software ABAQUS 6.14. The elastic buckling analysis and nonlinear analysis of cold-formed steel under axial load and beam-column actions are performed. The finite element model is validated with the test results. The finite element model is extended to other loading conditions also. CFS members are modelled using shell S4R elements. Based on the mesh convergence study, a mesh size of 5×5 mm is adopted. The mechanical properties from the coupon test result in the numerical model.

3.1 Loading and support condition

To simulate the warping restrained condition and loading at CG, multi point constraints (MPC) have been used, as shown in Fig. 12. The MPC constraint act similar to an endplate in the experiments. The simply supported boundary condition is applied at the MPC reference point.

The reference point is created according to the eccentricity needed based on the moment case required.

3.2 Analysis

The elastic buckling analysis gives the elastic critical load (P_{cr}) and buckling mode shape. The ultimate load is calculated using nonlinear analysis with static Rik's solution procedure. The strength of a CFS member is affected by the imperfections present in the members. Imperfection is applied as a combination of buckling modes as a result of buckling analysis with standard scaling factors. The imperfection factors suggested by (Schafer and Peköz, 1998) for the various buckling (**L** = 0.34t and **D**= 0.54t, **G** = l/1000) are used in this study. The nonlinear analysis is carried out for all the test specimen in order to compare them with the experimental results.

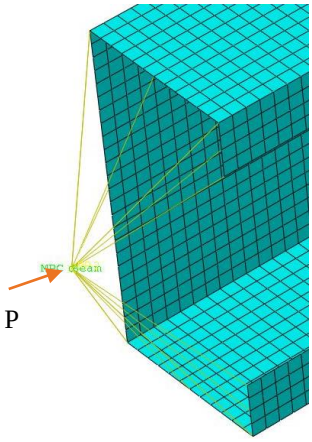

Figure 9: MPC constraints for warping restrained case

3.3 Validation of numerical study with experiments

The results from the numerical study on beam-columns are compared with the results of the experiment. The load and lateral deflection extracted from the numerical analysis are compared with the deflection from experiments. The deflection is measured at both the side of the flanges and the web as shown in Fig (4b). The load vs. lateral deflection curve for bi-axial compression is given in Fig. 10. The curve depicts that there is a constant increase in lateral-deflection at the mid-length of the web section. The difference in L2 and L3 is not much and follows a similar trend upto the ultimate load is reached. There is a deviation in L2 and L3 in the post-peak region which shows that there is a twist at the mid length of cross-section after reaching the ultimate load. Fig 10 shows that the numerical model can predict the beam-column behavior, and there is a reasonable match in the ultimate load with the results from experiments. Based on the validated model, the numerical model is extended for all the experimental loading conditions. A parametric study is performed for the prediction of ultimate strength under various biaxial eccentric loading conditions with a uniform moment and varying moment. The results of the parametric study is explained in the next section. The numerical results are compared with beam-column design expressions prescribed in AISI S100-2016 using (i) LI framework and (ii) NLI framework using DSM.

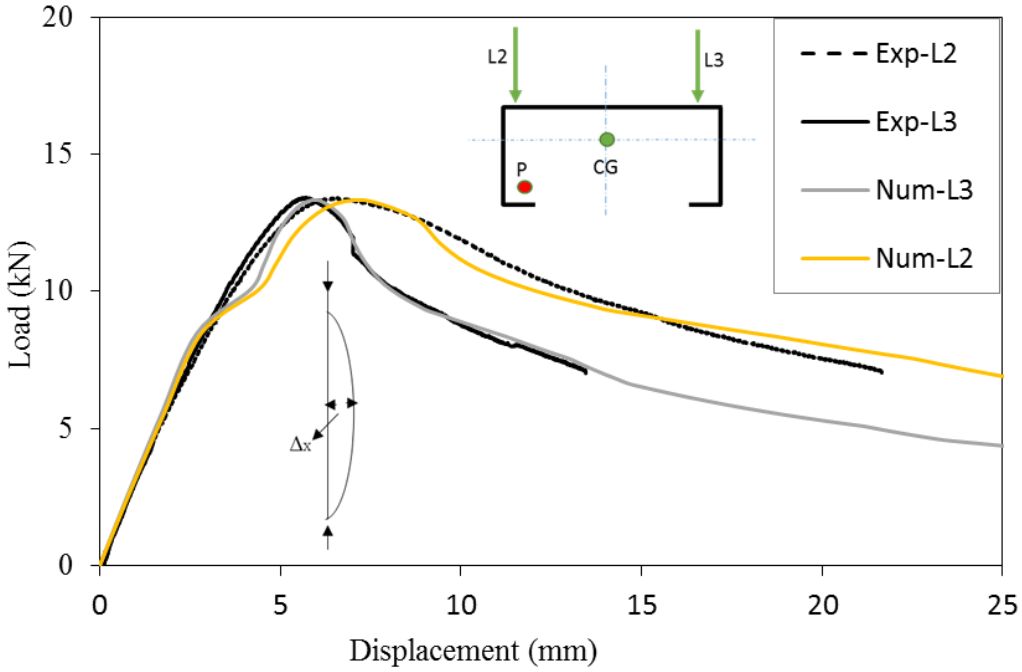

Figure 10: Validation of Numerical behaviour with experiment results

4. Comparision of Numerical results with DSM prediction

4.1 Nonlinear Beam-Column Interaction framework

The nonlinear interaction (NLI) framework for the design of beam-column is mainly based on the stability effects under actual combined stresses instead of considering individual stress action independently. In the NLI framework, the strength of the member is represented by a single parameter β_n, instead of three components of applied stress in the LI framework. The applied stress components are represented by β_r, θ_{mm}, and $\phi_{pm,}$ which is defined in Eq. (4), (5), and (6). The local buckling minima α_{crl} and distortional buckling minima α_{crd} from the signature curves for combined stresses have to be applied in Eq. (7).

$$\beta_r = \sqrt{x_r^{\,2} + y_r^{\,2} + z_r^{\,2}} \tag{4}$$

where $x_r = \frac{M_{r1}}{M_{y1}}, y_r = \frac{M_{r2}}{M_{y2}}, z_r = \frac{P_r}{P_y}$

$$\theta_{mm} = tan^{-1}\left(y_r / x_r\right) \tag{5}$$

$$\phi_{pm} = cos^{-1}\left(z_r / \beta_r\right) \tag{6}$$

$$\beta_{cr} = \alpha_{cr}\ \beta_r, \beta_y = \alpha_y\ \beta_r, \alpha_y = \frac{F_y}{F_{max}} \tag{7}$$

Where M_{r1}, M_{r2} is a resultant applied moment in major axis and minor axis direction including P-δ and P-Δ effect, and P_r is the applied axial load. DSM formula for beam and column is combined using Sine function, as shown in Eq. (8). This NLI framework is developed based on the uniform stress throughout the member.

$$\beta_{nG} = \beta_{nGP} + (\beta_{nGM} - \beta_{nGP}) \sin\phi_{PM} \quad (8)$$

The nonlinear interaction does not explicitly mention the moment gradient factor $C_{b,}$ and it conservatively assumes C_b as 1. In finite strip method, the analysis can be performed only for the uniform stress throughout the member. Thus, C_m and C_b assumed as 1 may result in the difference in the calculation of member capacities. The C_b factor and C_m factor specified in the design specification is developed based on the member subjected to bending alone. Thus, the effect of axial compression on the C_m and C_b factor is not considered. Thus, there is a need for the study in the area of defining the moment gradient factor in the NLI framework. The implication and effect of moment gradient factor in the NLI framework are studied in (Sevugan Rajkannu and Arul Jayachandran 2018). DSM based on CUFSM elastic buckling stress does not have a feature to consider the effect of warping on the buckling stress. The DSM prediction is based on the signature curve which is developed based on the simply supported and warping free boundary condition. In this study, the C_m factor given in Eq.2 is taken for both the axis.

4.2 Numerical results on biaxial loading with uniform moment

Numerical models are extended to a parametric study by varying the eccentricity so that the different combinations of the biaxial moment can be achieved. Two lengths of members (1600 mm and 600 mm) were selected for the numerical study with uniform and non-uniform moment along the length. For Intermediate length specimen (600 mm) alone yield stress is taken as 350 MPa. The numerical results are compared with the AISI S100 -2016 standard prediction for the beam-column member under biaxial-bending using DSM. The standard uses the linear interaction (LI) equation. The numerical results are also compared with the newly developed DSM based nonlinear interaction (NLI) framework. Table 4 shows the result for the 1600 mm length under biaxial bending with the uniform moment. The member under uniform moments makes the C_m=1 and C_b=1. The failures of the member are mostly within the elastic state, as shown in the experiment.

Table 4: Comparison of the numerical result of 1600 mm under uniform moment with LI and NLI

	e_x	e_y	P_{ult}	M_1	M_2					
ID	mm	mm	kN	kNmm	kNmm	P_{ult}/P_Y	M_1/M_{1y}	M_2/M_{2y}	LI	NLI
B-C1	-10.65	-30	32.50	-975.14	-346.17	0.38	-0.39	-0.31	1.89	1.21
B-C2	-0.65	-20	39.96	-799.12	-25.97	0.47	-0.32	-0.02	1.60	1.26
B-C3	9.35	-10	30.62	-306.19	286.29	0.36	-0.12	0.26	1.45	1.24
B-C4	14.35	-5	26.56	-132.79	381.11	0.31	-0.05	0.34	1.35	1.17
B-C5	19.35	0	22.97	0.00	444.47	0.27	0.00	0.40	1.25	1.11
B-C6	29.35	10	17.61	176.09	516.83	0.21	0.07	0.46	1.25	1.10
B-C7	36	35	13.34	466.94	480.28	0.16	0.19	0.43	1.20	1.04
B-C8	-35	35	23.59	825.62	-825.62	0.28	0.33	-0.74	2.07	1.22
B-C9	36	-35	14.08	-492.65	506.73	0.17	-0.20	0.45	1.27	1.11
B-C10	-35	-35	23.35	-817.22	-817.22	0.28	-0.33	-0.73	2.05	1.21

B-C11	30	30	15.07	452.24	452.24	0.18	0.18	0.40	1.22	1.05
B-C12	-30	30	26.09	782.70	-782.70	0.31	0.31	-0.70	2.10	1.22
B-C13	30	-30	15.89	-476.66	476.66	0.19	-0.19	0.43	1.29	1.34
B-C14	-30	-30	25.79	-773.58	-773.58	0.31	-0.31	-0.69	2.07	1.33
								Mean	1.58	1.19
								St.Dev	0.37	0.09

From the results of 1600 mm member (Table.3), it is clear that the LI framework conservatively predicts the strength of members with a mean of about 1.58 for the present numerical study. It is also noted that the standard deviation of LI prediction is also higher. However, the NLI framework predicts the strength of themember reasonably well with a mean of about 1.19, which reduces the conservatism of prediction. And the standard deviation of NLI prediction is also less when compared to the LI framework. Conservativeness in the LI framework is higher mainly in the case of negative eccentricity in the minor axis (i.e.) eccentric loading towards the shear center, which creates tension on the lip of the section. The numerical results of the 600 mm length specimen given in Table 5. Comparison of results show that the 600 mm length results also follow the same trend of conservatism as observed in 1600 mm length beam-column member results The Conservatism of interaction equation can be reduced by proper usage of M_{2ymax}, or M_{2ymin} recommended by the author (Vijay Vengadesh kumar and Arul Jayachandran 2016).

Table 5: Comparison of the numerical result of 600 mm under uniform moment with LI and NLI

ID	e_x	e_y	P_{ult}	M_1	M_2	P/P_Y	M_1/M_{1y}	M_2/M_{2y}	LI	NLI
	mm	mm	Kn	kNmm	kNmm					
B-I1	-10.65	-30	58.24	-1747.25	-620.28	0.47	-0.48	-0.38	1.74	1.26
B-I2	-0.65	-20	64.68	-1293.66	-42.04	0.53	-0.36	-0.03	1.28	1.19
B-I3	9.35	-10	57.94	-579.36	541.70	0.47	-0.16	0.33	1.35	1.28
B-I4	19.35	0	43.89	0.00	849.34	0.36	0.00	0.52	1.21	1.17
B-I5	-30.65	-50	38.51	-1925.29	-1180.20	0.31	-0.53	-0.72	1.91	1.28
B-I6	-40.65	-60	32.22	-1933.19	-1309.73	0.26	-0.53	-0.80	1.91	1.27
B-I7	-50.65	-70	27.41	-1918.99	-1388.52	0.22	-0.53	-0.85	1.89	1.25
B-I8	-60.65	-80	23.95	-1916.16	-1452.69	0.19	-0.53	-0.89	1.88	1.24
								Mean	1.65	1.24
								St.Dev	0.31	0.04

The conservatism in DSM prediction may also be due to difference in the warping end condition adopted in FSM and numerical results. The DSM centred on FSM results is developed based on warping free condition. Thus the effect of warping restraint on buckling all type buckling mode is neglected. The conservativeness can be reduced by appropriate modification on the DSM prediction, including warping restraint effects.

4.3 Numerical results on biaxial bending with moment gradient

The numerical model is extended to study the behaviour and ultimate strength effect on the beam-column due to the moment gradient. As similar to the uniform moment study, the two lengths of the member was selected. The ultimate strength from the numerical study is compared with the linear interaction (LI) framework and non-linear interaction (NLI) framework. The effect of moment gradient is taken care of by using Austin formula given in Eq.2 is used in both

the axis. The 1600 mm length was studied with a varying moment, similar to Fig (2 b) is performed. Load and boundary condition eccentricity concerning to centroid is given in Table 6. To create the moment gradient as shown in Fig (2b), the bottom end is loaded at the CG of the section. Table 6 shows the comparison of numerical results of 1600 mm length under biaxial bending with the varying moment. From the results of varying moment, it shows that the LI predicts conservatively with a mean of 1.52, and deviation along the result is 0.29. From Table 6, it is evident that the NLI framework predicts much better than LI. Since the DSM based on elastic buckling stress from the finite strip method (FSM) based software, which is developed based on uniform stress throughout the member. The effect of varying moments on DSM cannot be directly found. To take care of varying moments, the same parameter followed in the LI framework is followed by converting into an equivalent moment over the length using the C_m factor.

Table 6: Comparison of the numerical result of 1600 mm under varying moment Cm=0.6 with LI and NLI

	Eccentricity		ABAQUS							
ID	Top (e_x,e_y) mm	Bottom (e_x,e_y) mm	P_{ult} KN	M_1 kNmm	M_2 kNmm	P/P_Y	M_1/M_{1y}	M_2/M_{2y}	LI	NLI
B-V1	(-10.65,-30)	(0,0)	41.42	-1242	-441	0.50	-0.52	-0.42	1.96	1.29
B-V2	(-0.65,-20)	(0,0)	44.56	-891	-29	0.54	-0.38	-0.03	1.58	1.31
B-V3	(9.35,-10)	(0,0)	37.19	-372	348	0.45	-0.16	0.33	1.50	1.31
B-V4	(14.35,-5)	(0,0)	32.89	-164	472	0.40	-0.07	0.45	1.41	1.23
B-V5	(19.35,0)	(0,0)	29.14	0	564	0.36	0.00	0.54	1.31	1.16
B-V6	(29.35,10)	(0,0)	23.42	234	687	0.29	0.10	0.66	1.29	1.12
B-V7	(69.35,50)	(0,0)	12.77	638	885	0.16	0.27	0.85	1.20	1.06
B-V8	(-30.65,-50)	(0,0)	28.94	-1447	-887	0.35	-0.61	-0.85	1.94	1.16
								Mean	1.52	1.20
								St.Dev	0.29	0.10

For the moment gradient case given in Fig (2b), the maximum moment is converted into the equivalent moment by multiplying C_m=0.6 (for the given case) in both axes of bending. The application of C_b (moment correction factor) in the case of NLI is not properly defined. Thus the C_b is conservatively assumed as 1. For NLI prediction, the combined applied stress due to bending and compression, including the second order effect is applied. The result shows that NLI reduces the conservatism of prediction with a mean of 1.20 and a deviation of 0.1. The NLI prediction results are still conservative, which can be reduced by proper usage of the C_m factor. The proper usage of C_b can also decrease conservatism. The study is extended for different varying moment case also. Thus instead of the moment at the bottom end as zero, the moment is applied at the bottom end with the same sign as the moment at the top end of the member, which can change the C_m factor. The numerical result with different moment gradient cases is given in Table 7. C_m factor found based on Eq.2. From the result, it is evident that LI prediction is more conservative for members with moment gradient than the uniform moment. The LI framework prediction is conservative of about 80 to 100 percent for some cases, which shows there is a need for modification in the LI prediction. The NLI prediction is much better than LI prediction, but still, there is a chance for improvement in the varying moment cases.

Table 7: Comparison of numerical result of 1600 mm under varying moment with LI and NLI

ID	(e_x,e_y)/ (e_x,e_y) mm	C_{mx}	c_{my}	P_{ult} Kn	M_1 kNmm	M_2 kNmm	P/P_Y	M_1/M_{2y}	M_2/M_{2y}	LI	NLI
V2-C1	(-10,-30)/ (-5.65,-25)	0.81	0.93	34.43	-1033	-367	0.42	-0.44	-0.35	1.88	1.16
V2-C2	(-0.65,-20)/ (-5.65,-25)	0.65	0.92	38.64	-966	-218	0.47	-0.41	-0.21	1.71	1.16
V2-C3	(9.35,-10)/ (-5.65,-25)	0.40	0.76	38.20	-955	357	0.47	-0.40	0.34	1.70	1.25
V2-C4	(14.35,-5)/ (-5.65,-25)	0.44	0.68	34.06	-852	489	0.42	-0.36	0.47	1.67	1.23
V2-C5	(19.35,0)/ (-5.65,-25)	0.48	0.60	31.12	-778	602	0.38	-0.33	0.58	1.61	1.22
V2-C6	(29.35,10)/ (-5.65,-25)	0.52	0.40	25.79	258	757	0.31	0.11	0.73	1.22	1.11
V2-C7	(69.35,50)/ (-5.65,-25)	0.57	0.40	13.90	695	964	0.17	0.29	0.93	1.07	1.07
V2-C8	(-30,-50)/ (-5.65,-25)	0.67	0.80	26.63	-1332	-816	0.32	-0.56	-0.78	2.02	1.10
V2-C9	(-40,-60)/ (-5.65,-25)	0.66	0.77	23.13	-1388	-940	0.28	-0.59	-0.90	1.97	1.07
									Mean	1.65	1.15
									St.Dev	0.32	0.07

Numerical study on moment gradient is extended to intermediate length specimen of length 600 mm. The varying moment case given in Fig.2 b is created as a loading case. The results of the 600 mm length specimen for the C_m=0.6 moment gradient case are given in Table 8. The results are compared with the LI and NLI framework.

Table 8: Comparison of the numerical result of 600 mm under moment gradient (Cm=0.6) with LI and NLI

ID	Top		Bottom		P_{ult}	M_1	M_2					
	e_x mm	e_y mm	e_x mm	e_y mm	Kn	kN mm	kN mm	P/P_Y	M_1/M_{1y}	M_2/M_{2y}	LI	NLI
IV1	-10.65	-30	0	0	65.20	-1956	-694	0.53	-0.54	-0.43	1.49	1.14
IV2	-0.65	-20	0	0	76.60	-1532	-50	0.62	-0.42	-0.03	1.28	1.21
IV3	9.35	-10	0	0	70.43	-704	659	0.57	-0.19	0.40	1.33	0.95
IV4	19.35	0	0	0	56.08	0	1085	0.46	0.00	0.66	1.21	1.17
IV5	-30.65	-50	0	0	43.58	-2179	-1336	0.35	-0.60	-0.82	1.51	1.01
IV6	-40.65	-60	0	0	36.29	-2177	-1475	0.29	-0.60	-0.90	1.47	0.98
IV7	-50.65	-70	0	0	31.31	-2192	-1586	0.25	-0.60	-0.97	1.45	1.51
IV8	-60.65	-80	0	0	27.07	-2166	-1642	0.22	-0.60	-1.01	1.41	1.48
										Mean	1.40	1.18
										St.Dev	0.11	0.21

The members are predominantly failing in distortional and local buckling based on the loading condition. The effect of the moment gradient in the case of distortional or local is not much. The conservativeness of LI prediction for 600 mm length member is lesser than the longer length specimen. The change in conservatism may be due to the same moment correction factor for all the length of member independent of failure modes. From Table 7, It is important note that NLI framework overpredicts the strength of member for some of the loading case, and also NLI predicts the strength over-conservative than the LI for larger moment case. The results shows there is a need for the further study on the moment gradient effect in NLI framework.

5. Summary and conclusions

From the literature review, it is found that the experimental studies on cold-formed steel beam-column under biaxial bending is very less. A study is conducted on the lipped channel section under biaxial compression with uniform and gradient moment. The numerical model validated with the experimental result is used to study the members with different moment gradients. The results from this study are compared with AISI-S100 2016 beam-column DSM design expressions also with the NLI framework. Based on the present investigation, the following conclusions are derived.

The member capacities predicted for members under bi-axial bending with uniform moment shows that LI framework conservatively predicts the strength of member with a wide variation between 30% to 90%.

The conservativeness of LI framework is mainly in the region of eccentricity towards the shear center which creates tension on the lip of the section.

Numerical results of members with uniform moment in the intermediate length also follow the same degree of conservatism as longer length specimens. Capacities based on NLI are about 15% to 18% difference for long specimen.

The conservatism in the DSM predictions may be due to the warping end condition adopted in FSM and numerical results.

It is seen that, when the same moment correction factor is applied to all length, LI predictions are more accurate for intermediate length members than the longer length specimens.

Numerical results of intermediate length members under moment gradient shows that NLI overpredict the strength of member for some loading case. In case of larger moment gradient NLI predicts over-conservative than LI framework.

The Numerical results of members under moment gradient shows that there is a need for further investigations on defining the proper moment gradient factor in NLI framework.

6. References

AISI-S100. (2016). "North American Specification for the Design of Cold-Formed Steel Structural Members". Washington (DC, USA): *American Iron and Steel Institute*

Chen, W.F., Atsuta, T. (1976). "*Theory of Beam Columns*". McGraw-Hill International Book Company, New York.

Kalyanaraman, V., Jayabalan, P. (1994). "Local buckling of stiffened and unstiffened elements under nonuniform compression". International Specialty Conference on Cold-Formed Steel Structures: Recent Research and Developments in Cold-Formed Steel Design and Construction, 1–9.

Miller, T. H., Pekoz, T. (1994). "Load-eccentricity effects on cold-formed steel lipped-channel columns". Journal of Structural Engineering New York, N.Y., 120(3), 805–823.

Chen, W., & Zhou, S. (1988). Cm Factor in load and resistance factor design. Journal of Structural Engineering - ASCE, 113(8), 1738–1754.

Galambos, T. V. (1960). Report on the beam-column experiments. Wei-wen-yu center for cold-formed steel research, Missouri, United states.

Huang, Y., & Young, B. (2014). The art of coupon tests. Journal of Constructional Steel Research, 96, 159–175.

Li, Y. L., Li, Y. Q., Song, Y. Y., & Shen, Z. Y. (2016). In-plane behavior of cold-formed thin-walled beam-columns with lipped channel section. Thin-Walled Structures, 105, 1–15.

Pillai, S. U. (1981). An assessment of CSA standard equations for beam column design. Canadian Journal of Civil Engineering, 8(2), 130–136.

Put, B. M., Pi, Y.-L., & Trahair, N. S. (1999). Biaxial bending of cold-formed Z-beams. Journal of Structural Engineering, 125(11), 1284–1289.

Rasmussen, K. J. R. (2006). Design of slender angle section beam-columns by the Direct Strength Method, (February), 204–211.

Schafer, B. (2012). Development of DSM Direct Design Formulas for Beam-Columns. John hopkins university, USA.

Schafer, B. W., & Peköz, T. (1998). Computational modeling of cold-formed steel: characterizing geometric imperfections and residual stresses. Journal of Constructional Steel Research, 47(3), 193–210.

Sevugan Rajkannu, J., & Arul Jayachandran, S. (2018). Investigations on the Design implementation of cold-formed steel Beam-column Members Using Direct strength method. In Eighth International conference on Thin-Walled structures -ICTWS 2018 (Vol. 1, pp. 1–10). Lisbon, Portugal.

Sevugan Rajkannu, J., & Arul Jayachandran, S. (2019). Investigation on the effect of warping on the stability behaviour of cold formed steel beam-columns. In Annual stability conference Structural Stability Research Council (SSRC) (pp. 902–920). St. Louis, Missouri, U.S.A.,.

Shanmugam, N. E., Liew, J. Y. R., & Lee, S. L. (1989). Thin-walled steel box columns under biaxial loading. Journal of Structural Engineering New York, N.Y., 115(11), 2706–2726.

Sohal, I. S., Duan, L., & Chen, W. (1989). Design Interaction equations for steel members. Journal of Structural Engineering, 115(7), 1650–1665.

Talebian, N., Gilbert, B. P., Pham, C. H., Chariere, R., & Karampour, H. (2018). Local and Distortional Biaxial Bending Capacities of Cold-Formed Steel Storage Rack Uprights. Journal of Structural Engineering (United States), 144(6), 1–15.

Torabian, S., Fratamico, D. C., & Schafer, B. W. (2015). Experiments on cold-formed steel Zee-shaped stub beam-columns. Structural Stability Research Council Annual Stability Conference 2015, SSRC 2015, 1–18.

Torabian, S., Zheng, B., & Schafer, B. W. (2014). Experimental study and modeling of cold-formed steel lipped channel stub beam-columns. In Structural Stability Research Council Annual Stability Conference 2014, SSRC 2014 (pp. 380–401).

Vijayavengadesh Kumar, J., Arul Jayachandran, S. (2016). "Experimental investigation and evaluation of Direct Strength Method on beam-column behavior of uprights". *Thin-Walled Structures*, *102*, 165–179.